

NJC

Accepted Manuscript



This is an *Accepted Manuscript*, which has been through the Royal Society of Chemistry peer review process and has been accepted for publication.

Accepted Manuscripts are published online shortly after acceptance, before technical editing, formatting and proof reading. Using this free service, authors can make their results available to the community, in citable form, before we publish the edited article. We will replace this *Accepted Manuscript* with the edited and formatted *Advance Article* as soon as it is available.

You can find more information about *Accepted Manuscripts* in the [Information for Authors](#).

Please note that technical editing may introduce minor changes to the text and/or graphics, which may alter content. The journal's standard [Terms & Conditions](#) and the [Ethical guidelines](#) still apply. In no event shall the Royal Society of Chemistry be held responsible for any errors or omissions in this *Accepted Manuscript* or any consequences arising from the use of any information it contains.

Cite this: DOI: 10.1039/c0xx00000x

www.rsc.org/xxxxxx

ARTICLE TYPE

A facile preparation route for highly conductive borate cross-linked reduced graphene oxide paper

Zhengshan Tian^{a, b}, Chunxiang Xu^{*a}, Jitao Li^a, Gangyi Zhu^a, Jing Wu^a, Zengliang Shi^a, Yueyue Wang^a

Received (in XXX, XXX) XthXXXXXXXXXX 20XX, Accepted Xth XXXXXXXXXXXX 20XX

DOI: 10.1039/b000000x

A facile hydrothermal strategy to synthesize borate cross-linked reduced graphene oxide (B-RGO) sheets with good optical and electrical properties is proposed by using graphene oxide (GO) sheets, boric acid and sodium hydroxide as precursors in one pot without any polymer or surfactant. The resulting B-RGO sheets can be assembled into highly conductive B-RGO paper by a simple filtration. Moreover, the atomic percentage of boron (B) in the B-RGO sheet can be readily controlled, as it reaches to the maximum of 3.33 At%, about 30.0 mA current passes through the resulting single-layer B-RGO sheet and B-RGO paper at an applied bias of 2.0 V. The value of current is much higher than that of the annealed GO paper (~ 1.2 mA), and very close to that of the single-layer graphene sheet (~ 60.0 mA) synthesized by chemical vapor deposition method under the same test conditions. The resulting highly conductive B-RGO sheet and B-RGO paper will provide a promising transparent conductive material for electronic or optoelectronic applications.

Introduction

As a two-dimensional (2D) monolayer form of sp^2 and sp^3 hybridized carbon atoms linked covalently with oxygen-containing groups,^{1, 2} GO sheet has now become a more promising basic building block to fabricate multi-functional graphene-based derivatives because of its low cost, easy preparation, scalable production, high processability, and dispersibility in water and polar organic solvents,³ besides it traditionally served as a precursor for graphene. Abundant oxygen-containing functional groups in the basal plane and at the edges of GO sheet permit many active interactions between GO sheet and various organic/inorganic materials in non-covalent, covalent and/or ionic manners^{4, 5} to create graphene-based derivatives with unusual properties.⁶ Based on these interactions, GO sheets have been assembled into different macroscopic 2D thin films,⁷⁻¹⁰ membranes,¹¹ and other networks¹² for the desired applications as transparent electrodes, chemical filters, electronic papers,^{4, 13, 14} and molecular storage. For example, Dikin *et al.* prepared GO paper with good flexibility and stiffness by flow-directed assembly of individual GO sheets dispersed in water.⁴ Chen *et al.* synthesized free-standing GO membranes with excellent mechanical and optical performances at the liquid/air interface.¹¹ However, these large-area 2D GO-based materials have the deficient electrical conductivity for wide applications. Although chemical vapour deposition (CVD) method provides a promising way to synthesize large-area high-quality single-layer or few-layer graphene film¹⁵ with excellent conductivity, the high cost of graphene film synthesized by a CVD method hinders its

further application. Fortunately, great endeavor has been paid on 2D GO-based materials to improve their electrical conductivity.^{7, 12, 13} For example, Chen *et al.*¹³ synthesized the conductive graphene paper by controlling reduction of GO dispersions with hydrazine. Cheng and his collaborators¹⁶ used hydrohalic acid as a reducing agent to reduce GO films into highly conductive graphene films based on the nucleophilic substitution reaction. However, the usage of toxic reagents also limits the development and application of GO-based materials. The conductivity of GO film/paper can be rendered by hydrogen reduction or simple thermal annealing under high temperature but the structure and mechanical properties of GO film/paper are generally deteriorated after these treatments. Recent reported chemical modification^{14, 17-19} provided an effective method to tailor the intrinsic properties of GO-based materials by boron or nitrogen doping and molecular cross-linking.²⁰⁻²² Sheng *et al.*²³ reported a catalyst-free approach to synthesize boron-doped graphene by thermal annealing graphite oxide in the presence of B_2O_3 at 1200 °C for 4 h and found its excellent electrocatalytic activity towards an oxygen reduction reaction. Though various methods^{23, 24} have been employed to prepare boron-doped/modified GO sheets, the required higher temperature, special apparatus and rigorous conditions limited their scale-up production. Furthermore, the electrical conductivity of most reported chemically-modified GO-based materials are still too low to enable them for practical applications. Therefore, a facile fabrication of highly conductive single-layer/few-layer GO-based film or large-area GO-based paper would still be of both scientific and technological

importance for practical applications. A simple and convenient borate cross-linking strategy to improve dramatically the electrical properties of GO sheet and large-area GO paper still lacks, and it is strongly desired.

In this paper, a facile borate cross-linking strategy was proposed to synthesize B-RGO sheets by using GO sheets, boric acid (H_3BO_3) and sodium hydroxide (NaOH) as precursors through a mild hydrothermal reaction process in one pot. Then, the resulting B-RGO sheets dispersed in water were assembled into B-RGO paper by a simple filtration. During the hydrothermal reaction process, the introduced borate ions acted as a cross-linking agent to patch up the hole defects in the basal plane of GO sheet, and NaOH caused GO sheet to undergo quick deoxygenation in alkali solution at moderate temperature. The synergistic effects of the cross-linking agent and the deoxygenation agent further result in the dramatical improvement for the electrical properties of the resulting B-RGO sheets and B-RGO paper.

Experimental Section

Preparation of the Samples

The B-RGO sheets were synthesized by using GO sheets, H_3BO_3 and NaOH as precursors through a hydrothermal reaction process at 90 °C in one pot. Subsequently, the resulting B-RGO sheets dispersed in water were assembled into B-RGO paper through a filter. Firstly, without any polymer or surfactant, a homogeneous GO aqueous solution (3 mg/mL) was obtained by controlling ultrasonication-assisted exfoliation of graphite oxides, which were synthesized from graphite powders based on a modified Hummers' method.²⁵ Then, a given amount of H_3BO_3 was introduced into the GO aqueous solution under magnetic stirring at 25 °C for 10 min, and an appropriate amount of NaOH aqueous solution (4 M) was also added into the aforementioned mixture to adjust the pH value to 12, subsequently heated to 90 °C and maintained at this temperature for 3 h to obtain a dispersion containing B-RGO sheets. Thirdly, the dispersion containing B-RGO sheets was naturally cooled to room temperature, purified by filtration, washed with deionized water several times, and re-dispersed in deionized water by ultrasonication. Finally, the B-RGO paper was fabricated by filtration of a given amount of B-RGO aqueous solution (2 mg/mL) through an Anodisc membrane filter (80 mm in diameter, 0.2 μm pore size, Whatman), followed by air drying, and peeled from the filter. The atomic percentage of B (0-3.33 At%) in the resulting B-RGO sheets was readily controlled by adjusting the initial amount of H_3BO_3 in the parent mixture solution. The thickness of each B-RGO paper sample was controlled by adjusting the volume of the B-RGO aqueous solution. For comparison, the GO paper was prepared by using a similar procedure. The annealed GO paper was obtained by transferring the GO paper into a Teflon-lined stainless steel autoclave (100 mL), heated to 200 °C and maintained at this temperature for 10 h. The RGO paper was also synthesized under the same condition as that of B-RGO paper without adding H_3BO_3 . A single-layer graphene sheet was synthesized by a CVD method.²⁶

Characterization

The morphologies and structures of the samples were characterized by a scanning electron microscope (SEM, Hitachi S-4800) equipped with energy dispersive X-ray spectroscopy (EDX), a transmission electron microscope (TEM, JEM-2100), and a X-ray diffractometer (XRD, Bruker D8 Discover) with Cu K α radiation (1.5406 Å). Raman spectrum with an excitation laser of 514.5 nm (LabRAM HR800), X-ray photoelectron spectroscopy (XPS, ESCALAB 250Xi) and Fourier transform infrared spectrum (FTIR, Nicolet5700) were also used to analyze the components and the formation process of the samples.

Optical and Electrical Experiments

For optical tests, the B-RGO sheets (B atomic percentage is 3.33 At%) dispersed in deionized water were spin-coated onto the glass substrates (2 cm \times 2 cm) to form B-RGO films. A series of B-RGO films with thicknesses of about 10 nm, 15 nm, and 20 nm were assembled, respectively. The thicknesses of B-RGO films were measured by observing the cross-sections in a SEM. The absorption and transmittance spectra of the B-RGO films with different thicknesses were measured on a spectrophotometer (UV-2600).

To facilitate and test the electrical performance of the samples, GO paper, annealed GO paper, RGO paper, B-RGO sheets, B-RGO paper and a single-layer graphene of CVD were firstly floated on the surface of deionized water, then transferred onto the interdigitated Au electrodes (about 30 μm intervals on rigid ceramic substrate), and dried in a vacuum oven at 60 °C for 4 h, respectively. The electrical conductivities of the samples transferred onto the interdigitated Au electrodes were measured by a semiconductor parameter analyzer (KEITHLEY 4200-SCS) with a two electrode system.

Results and Discussion

TEM and SEM Characterizations

A homogeneous GO aqueous solution is readily prepared by controlling ultrasonication-assisted exfoliation of graphite oxides in deionized water without any polymer or surfactant. Figure 1 shows the detailed nanoscale morphologies of GO sheets before and after borate cross-linking by a TEM. The TEM images of the parent GO sheets offer an immediate evidence of the peeled-off GO sheets through the Hummers' process and the ultrasonic exfoliation process. These as-prepared GO sheets are mostly a monolayer or few-layers, individually well-dispersed in deionized water, because of the electrostatic repulsion of the surface charge.²⁷ Figure 1a demonstrates GO sheets with some distinct folds and wrinkling, because abundant functional groups of GO sheet disrupt the original conjugation and result in folds and distortions on the surface of GO sheet.²⁸ Compared with the GO sheets with few-layers in Figure 1a, Figure 1b reveals that B-RGO sheets with few-layers have much more 'waviness', presumably due to the induced contraction of borate cross-linking in the basal plane of B-RGO sheet, which look like many repair traces on the surface of B-RGO sheet. Figure 1d more clearly shows some repair traces on a wavy B-RGO sheet with a monolayer, which is very different from a monolayered GO sheet in Figure 1c. The corresponding selected area electron diffraction (SAED) pattern obtained in TEM shows the signature of a few-

layered sheet (Figure 1e), and the other SAED pattern shown in Figure 1f confirms the hexagonal pattern of a monolayered sheet.

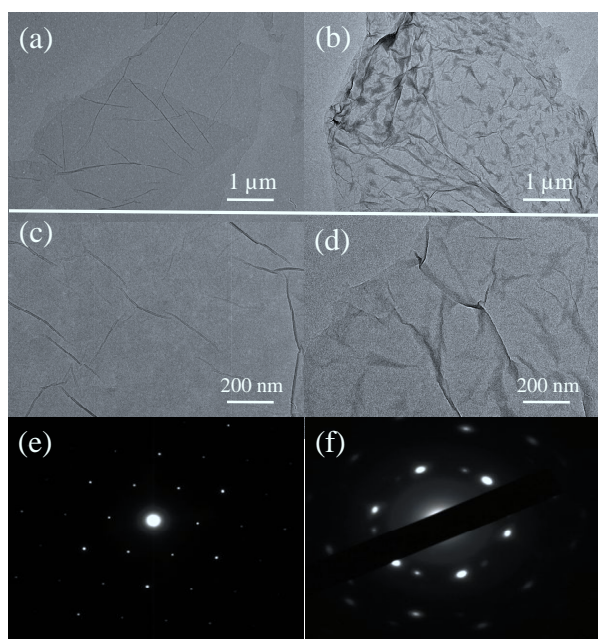


Fig. 1 (a, b) TEM images of few-layered GO sheets before and after borate cross-linking, (c, d) TEM images of a monolayered GO sheet before and after borate cross-linking, and (e, f) The SAED patterns of a few-layered sheet and a monolayered sheet.

Figure 2a shows an optical photograph of the self-supporting brown-black thin B-RGO paper, which is readily removable from the membrane for characterization. A high-magnification SEM image (Figure 2b) of the surface of B-RGO paper clearly shows the 'patch-like' 'waviness' structure throughout the entire surface of B-RGO paper. The fractured edges of B-RGO paper exhibit a layered structure through the entire cross-section (Figure 2c and 2d), similar to those of graphene and GO papers recently reported in the literature.^{4, 11, 13}

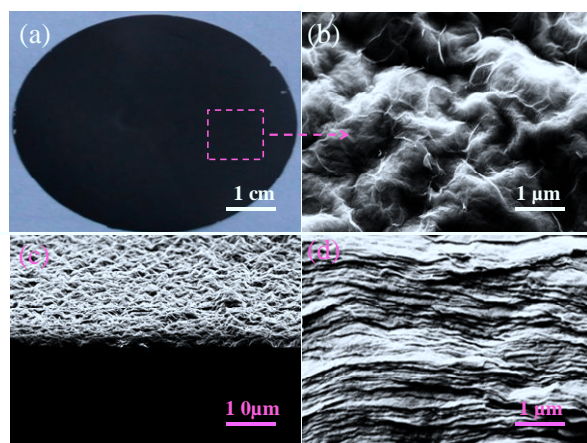


Fig. 2 (a) Optical photograph of B-RGO paper, (b) SEM image of the B-RGO paper surface, and (c, d) SEM images of the cross-section of B-RGO paper with different magnifications.

Formation Mechanism Analysis

To further probe the formation mechanism of the 'patch-like' structure of B-RGO sheet, some important features of the chemical structure of GO sheet shall be briefly described below.

Oxygen-containing functional groups and other hole defects are inevitably formed in GO sheet because of the harsh oxidation in the Hummers' process.²⁹ The atomic structure of GO sheet is a disrupted planar π -network structure,^{2, 5} which exhibits phenol hydroxy and epoxide groups in the basal plane, and carboxylic groups at the lateral edges of GO sheet. Abundant oxygen-containing functional groups create chemically reactive sites to allow the interactions between GO sheet and various organic/inorganic materials in non-covalent, covalent and/or ionic manners.^{4, 5}

During the hydrothermal reaction process of 90 °C in one pot, H_3BO_3 was transformed into borate ions in an alkali NaOH aqueous solution. It is assumed that the borate ions play a key role in the formation of B-RGO sheet based on the morphological evolution from GO sheet to B-RGO sheet. In other words, the borate ions can patch up the hole defects in the basal plane of GO sheet by cross-linking during the hydrothermal reaction.^{22, 30} The formation of covalent bonds between the borate ions and the hydroxyl groups of GO sheet is similar to the borate cross-links in plants, which occur through hydroxymethyl moieties on structural elements in their cell walls.³¹

To confirm the incorporation of the borate ions into the B-RGO sheet, the elemental analyses of the sample (Figure 3a) via EDX was used to disclose the presence of carbon (C), oxygen (O) and boron (B). When the amount of H_3BO_3 in the parent reaction solution was largely excessive, the atomic percentage of B in the B-RGO sheets could reach to a maximum of 3.33 At%, accompanied with C of 65.60 At% and O of 31.07 At%, as shown in Figure 3b. The C atoms originate from the framework of GO sheet, the O atoms come from oxygen-containing functional groups of GO sheet, and the B atoms only originate from the borate ions cross-linked in the B-RGO sheets.^{22, 30} The elemental mappings (Figure 3c-e) of the selected region reveal the distribution of the C, O and B atoms in the B-RGO paper, particularly the uniform distribution of B atoms.

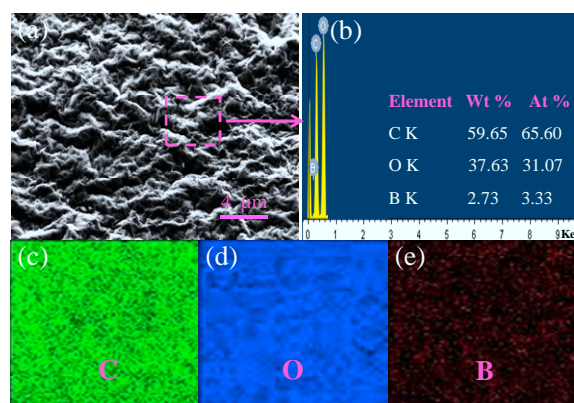


Fig. 3 (a) SEM image of B-RGO paper, (b) Elemental analysis aided by EDX, and (c-e) Elemental mapping of the selected region of B-RGO paper.

The compositional analysis by the XPS survey spectra reveals that GO sheets initially exhibited a considerably high oxygen signal. It is worth to note that the O1s peak shows an apparent decrease after borate cross-linking (Figure 4a), and a weak XPS

signal from the B1s peak appears. The B1s peak would present an obvious change with different B atomic percentage in the B-RGO sheets. The high resolution B1s peak in the B-RGO sheets mainly contains two components centered at 191.6 eV and 192.1 eV (Figure 4b), both of them have a higher binding energy compared with 187 eV for pure boron. The binding energy peaked at 191.6 eV corresponds to the boron atoms bonding to carbon and oxygen atoms (BC₂O), and the other peak at 192.1 eV corresponds to the boron atoms surrounded by carbon and oxygen atoms (BCO₂).²³ The high resolution C1s spectrum of the original GO sheet (Figure 4c) reveals the presence of C=C/C-C (~ 284.7 eV), C-O (hydroxyl and epoxy, ~ 285.8 eV), C=O (carbonyl, ~ 286.7 eV), and O-C=O (carboxyl, ~ 288.4 eV) groups.¹⁶ The C1s XPS spectrum of B-RGO sheet (Figure 4d) also shows an apparent decrease of oxygen-containing functional groups compared with that of GO sheet in Figure 4c, suggesting that the borate ions can react with GO sheet. Therefore, the XPS analyses support our aforementioned hypothesis.

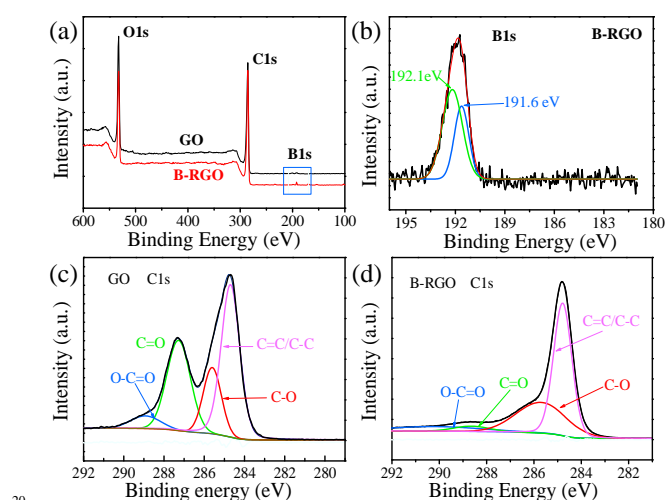


Fig. 4 (a) XPS survey spectra of GO sheet and B-RGO sheet, (b) High-resolution XPS spectra of the B1s region for B-RGO sheet, (c, d) High-resolution XPS spectra of the C1s region for GO sheet and B-RGO sheet.

The XRD patterns of the pristine GO sheets and the resulting B-RGO sheets are shown in Figure 5a. For the pristine GO sheets, a strong diffraction peak appears at $2\theta = 10.10^\circ$, which corresponds to an interlayer spacing of $\sim 8.75 \text{ \AA}$. For the B-RGO sheets, the XRD patterns exhibit an intense peak at $2\theta = 10.40^\circ$ corresponding to the interlayer spacing of $\sim 8.50 \text{ \AA}$.¹⁶ It is noted that a relatively weak peak appears at $2\theta = 26.20^\circ$ corresponding to the interlayer spacing of $\sim 3.40 \text{ \AA}$ for the partial restoration of sp² carbon,³² which is very close to the d-spacing of the (002) crystal plane of graphite (3.35 \AA). The XRD results indicate the efficient structural restoration of the graphitic framework during the hydrothermal reaction process.

Raman and FTIR analyses are also performed on the pristine GO sheets and the resulting B-RGO sheets. Both a D peak ($\sim 1350 \text{ cm}^{-1}$) and a G peak ($\sim 1595 \text{ cm}^{-1}$) are presented in the Raman spectra of GO sheets and B-RGO sheets in Figure 5b. The intensity ratio of the D band ($\sim 1350 \text{ cm}^{-1}$) to the G band ($\sim 1595 \text{ cm}^{-1}$) (I_D/I_G) decreases from 1.03 for GO sheets to 0.93 for B-

RGO sheets, suggesting a part restoration of the graphitic framework.³³ The FTIR spectra of the pristine GO sheets (Figure 5c) have proved the presence of different functional groups, such as O-H stretching vibration around 3340 cm^{-1} , C-H stretching vibration around 2971 cm^{-1} and 1385 cm^{-1} , C=O stretching mode at 1740 cm^{-1} , C=C stretching vibration around 1645 cm^{-1} , C-OH stretching vibration at 1250 cm^{-1} , and C-O stretching mode at 1050 cm^{-1} . In addition, the relative intensities of O-H, C=O, C-H, C-OH, and C-O decrease dramatically from the pristine GO sheets to the resulting B-RGO sheets, also implying that the degree of sp² domains in the B-RGO sheets appears an apparent increase.³⁴

Based on the EDX, XPS, XRD, Raman and FTIR analyses mentioned above, it is reasoned that the borate ions can act as cross-linking agent to patch up the GO sheets in the basal plane through cross-linking interactions. On the other hand, the GO sheets can undergo quick deoxygenation in NaOH aqueous solution at moderate temperature in the hydrothermal reaction process, similar to recent reports in the literature.^{35, 36}

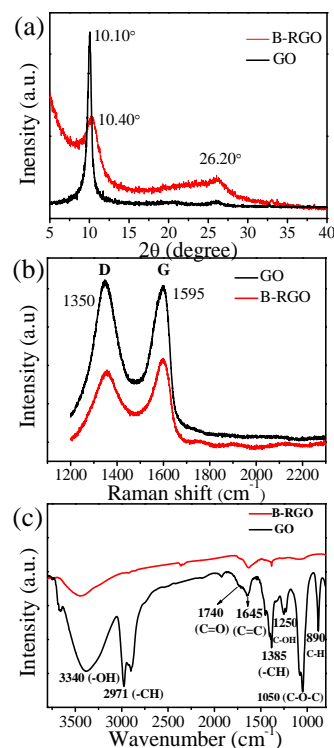


Fig. 5 (a) XRD patterns of GO sheet and B-RGO sheet, (b) Raman spectra of GO sheet and B-RGO sheet, and (c) FTIR spectra of GO sheet and B-RGO sheet.

Optical and Electrical Property

A series of optical photographs of the B-RGO films with different thicknesses ($\sim 10 \text{ nm}$, 15 nm , and 20 nm) are shown in the inset of Figure 6a. "SEU" (the abbreviation of Southeast University) under the B-RGO films is seen clearly, suggesting a transparent feature of these films. Figure 6a shows the absorption spectra of the B-RGO films in the range of $200 \sim 900 \text{ nm}$. The transmittance spectra in Figure 6b show a good transmittance of the B-RGO films with different thicknesses in the visible region, and their

values are very close to those of the graphene films.^{9, 37-39} Figure 6c displays a B-RGO sheet transferred onto the interdigitated Au electrodes with about 30 μm intervals. The Raman spectrum (inset of Figure 6c) shows that the 2D peak and G peak are very sharp Lorentzian lineshape with the intensity ratio of the 2D band to the G band (I_{2D}/I_G) \approx 2, while the defect related D peak is very weak. This indicates that the B-RGO sheet transferred onto the Au electrodes is almost a monolayer, consistent with the observations of the SEM image in Figure 6c and the TEM image in Figure 1d. Its current-voltage (I-V) curve in Figure 6d exhibits a very high current reaching \sim 30.0 mA at an applied bias of 2.0 V, indicating its excellent electrical property.

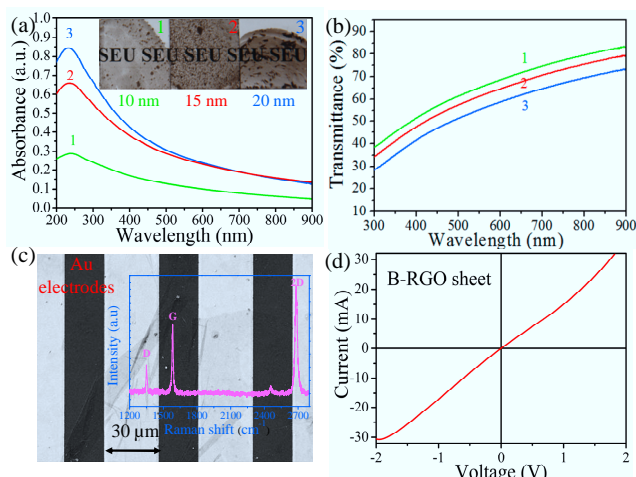


Fig. 6 (a) Absorption spectra of the B-RGO films, the insets are a series of optical photographs of the B-RGO films with different thicknesses (\sim 10 nm, 15 nm, and 20 nm). (b) Optical transmittance curves of the B-RGO films, (c) SEM image of the B-RGO sheet transferred onto the interdigitated Au electrodes with about 30 μm intervals, the inset is the Raman spectrum of a single-layer B-RGO sheet, and (d) I-V curve of a single-layer B-RGO sheet.

The resulting B-RGO paper also showed high conductivity, which was confirmed by two terminal I-V measurements (Figure 7). For comparison, the electrical conductivities of a GO paper, an annealed GO paper at 200 $^{\circ}\text{C}$ and a single-layer CVD-grown graphene sheet were also measured. The I-V curve of the GO paper exhibits a very low current of about 2.5 μA at a high applied bias of 5.0 V (Figure 7a), indicating that the GO paper is almost electrically insulating. The electrical conductivity of the B-RGO paper enhances with the increasing atomic percentage of B (0-3.33 At%), as shown in Figure 7b. As the atomic percentage of B reaches to the maximum of 3.33 At%, about 30.0 mA current passes through the resulting B-RGO paper at an applied bias of 2.0 V. Its value of current is much higher than that of the annealed GO paper (\sim 1.2 mA), and very close to that of the CVD-made single-layer graphene (\sim 60.0 mA) at the same applied bias (Figure 7c-d). The difference between the conductivity of the GO sheet and the graphene sheet is mainly ascribed to the breakthrough of conductive sp^2 network in the graphene sheet by replacement of some sp^3 carbon sites.^{40, 41}

Based on the EDX, XPS, XRD, Raman and FTIR analyses mentioned above, it is reasoned that the borate ions can act as a

cross-linking agent to patch up the B-RGO sheet in the basal plane, and NaOH can cause the B-RGO sheet to undergo quick deoxygenation in alkali solution to restore a part of the graphitic framework in the hydrothermal reaction process. The synergistic effects of the borate ions and NaOH enhance dramatically the electrical conductivities of the resulting B-RGO sheets and the B-RGO paper.^{32, 40}

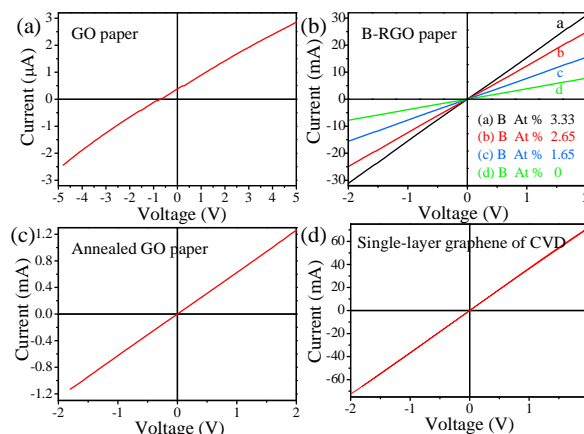


Fig. 7 I-V curves of (a) GO paper, (b) B-RGO papers with different B atomic percentage, (c) an annealed GO paper, and (d) a single-layer graphene of CVD.

Conclusion

In this work, we demonstrated the facile synthesis of borate cross-linked reduced graphene oxide sheets by using graphene oxide sheets, boric acid and sodium hydroxide as precursors through a mild hydrothermal reaction process at 90 $^{\circ}\text{C}$ in one pot without any polymer or surfactant. The resulting borate cross-linked reduced graphene oxide sheets with good optical and electrical properties were assembled into highly conductive graphene-based paper by a simple filtration. Moreover, as the atomic percentage of B reaches to the maximum of 3.33 At%, about 30.0 mA current passes through the resulting single-layer borate cross-linked reduced graphene oxide sheet and the resulting paper at an applied bias of 2.0 V. The value of current is much higher than that of the annealed graphene oxide paper (\sim 1.2 mA), and very close to that of the single-layer graphene sheet made by chemical vapor deposition (\sim 60.0 mA) under the same test conditions. During the hydrothermal reaction process, the introduced borate ions acted as a cross-linking agent to patch up the hole defects in the basal plane of the graphene oxide sheet, and sodium hydroxide caused the graphene oxide sheet to undergo quick deoxygenation in alkali solution at moderate temperature. The synergistic effects of the cross-linking agent and the deoxygenation agent improve dramatically the electrical properties of the resulting borate cross-linked reduced graphene oxide sheets and the resulting paper. This result shows that the resulting borate cross-linked reduced graphene oxide sheets and the resulting paper will provide many technological applications such as transparent electrodes, protective layers, components of electrical batteries or supercapacitors, electronic

or optoelectronic components.

Acknowledgements

This work was supported by NSFC (61475035 and 11404289), “973” Program (2013CB932903 and 2011CB302004), and the Scientific Research Foundation of Graduate School of Southeast University (YBJJ1315) in China.

Notes and references

^aState Key Laboratory of Bioelectronics, School of Biological Science and Medical Engineering, Southeast University, Nanjing 210096, P. R. China.

^bSchool of Chemistry and Chemical Engineering, Pingdingshan University, Pingdingshan 467000, P. R. China.

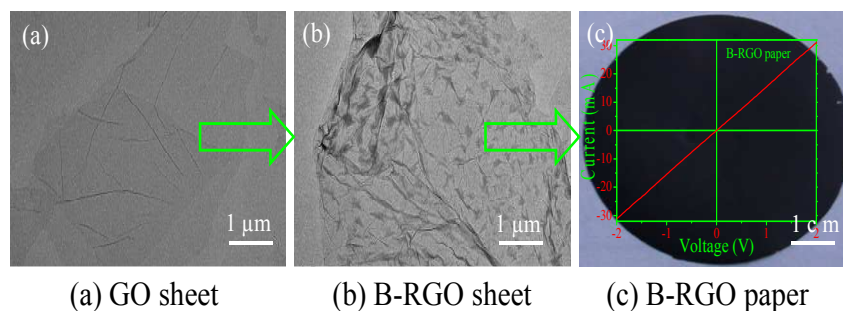
* Corresponding Author: E-mail: xcxseu@seu.edu.cn

1. Y. Zhu, S. Murali, W. Cai, X. Li, J. W. Suk, J. R. Potts, and R. S. Ruoff, *Adv. Mater.*, 2010, **22**, 3906-3924.
2. K. P. Loh, Q. Bao, G. Eda, and M. Chhowalla, *Nat. Chem.*, 2010, **2**, 1015-1024.
3. Z. Xu, and C. Gao, *Nat. Commun.*, 2011, **2**, 571.
4. D. A. Dikin, S. Stankovich, E. J. Zimney, R. D. Piner, G. H. Dommett, G. Evmenenko, S. T. Nguyen, and R. S. Ruoff, *Nature*, 2007, **448**, 457-460.
5. K. Erickson, R. Erni, Z. Lee, N. Alem, W. Gannett, and A. Zettl, *Adv. Mater.*, 2010, **22**, 4467-4472.
6. L. Liu, Z. Niu, L. Zhang, and X. Chen, *Small*, 2014, **10**, 2200-2214.
7. F. Gunes, H. J. Shin, C. Biswas, G. H. Han, E. S. Kim, S. J. Chae, J. Y. Choi, and Y. H. Lee, *ACS Nano*, 2010, **4**, 4595-4600.
8. F. Liu, and T. S. Seo, *Adv. Funct. Mater.*, 2010, **20**, 1930-1936.
9. K. S. Kim, Y. Zhao, H. Jang, S. Y. Lee, J. M. Kim, K. S. Kim, J. H. Ahn, P. Kim, J. Y. Choi, and B. H. Hong, *Nature*, 2009, **457**, 706-710.
10. X. Yang, C. Cheng, Y. Wang, L. Qiu, and D. Li, *Science*, 2013, **341**, 534-537.
11. C. Chen, Q.-H. Yang, Y. Yang, W. Lv, Y. Wen, P.-X. Hou, M. Wang, and H.-M. Cheng, *Adv. Mater.*, 2009, **21**, 3007-3011.
12. S. H. Lee, H. W. Kim, J. O. Hwang, W. J. Lee, J. Kwon, C. W. Bielawski, R. S. Ruoff, and S. O. Kim, *Angew. Chem. Int. Ed.*, 2010, **49**, 10084-10088.
13. H. Chen, M. B. Müller, K. J. Gilmore, G. G. Wallace, and D. Li, *Adv. Mater.*, 2008, **20**, 3557-3561.
14. S. Park, K. S. Lee, G. Bozoklu, W. Cai, S. T. Nguyen, and R. S. Ruoff, *ACS Nano*, 2008, **2**, 572-578.
15. S. Bae, H. Kim, Y. Lee, X. Xu, J.-S. Park, Y. Zheng, J. Balakrishnan, T. Lei, H. R. Kim, Y. I. Song, Y.-J. Kim, K. S. Kim, B. özyilmaz, J.-H. Ahn, B. H. Hong, and S. Iijima, *Nat. Nanotech.*, 2010, **5**, 574-578.
16. S. Pei, J. Zhao, J. Du, W. Ren, and H.-M. Cheng, *Carbon*, 2010, **48**, 4466-4474.
17. H. Liu, Y. Liu, and D. Zhu, *J. Mater. Chem.*, 2011, **21**, 3335-3345.
18. P. Marconcini, A. Cresti, F. Triozon, G. Fiori, B. Biel, Y. M. Niquet, M. Macucci, and S. Roche, *ACS Nano*, 2012, **6**, 7942-7947.
19. Z. H. Sheng, L. Shao, J. J. Chen, W. J. Bao, F. B. Wang, and X. H. Xia, *ACS Nano*, 2011, **5**, 4350-4358.
20. W. Cui, M. Li, J. Liu, B. Wang, C. Zhang, L. Jiang, and Q. Cheng, *ACS Nano*, 2014, 10.1021/nn503755c.
21. J. Wu, H. Li, X. Qi, Q. He, B. Xu, and H. Zhang, *Small*, 2014, **10**, 2239-2244.
22. Z. An, O. C. Compton, K. W. Putz, L. C. Brinson, and S. T. Nguyen, *Adv. Mater.*, 2011, **23**, 3842-3846.
23. Z.-H. Sheng, H.-L. Gao, W.-J. Bao, F.-B. Wang, and X.-H. Xia, *J. Mater. Chem.*, 2012, **22**, 390-395.
24. Z.-S. Wu, W. Ren, L. Xu, F. Li, and H.-M. Cheng, *ACS Nano*, 2011, **5**, 5463-5471.
25. W. S. Hummers, and R. E. Offeman, *J. Am. Chem. Soc.*, 1958, **80**, 1339-1339.
26. X. Li, W. Cai, J. An, S. Kim, J. Nah, D. Yang, R. Piner, A. Velamakanni, I. Jung, E. Tutuc, S. K. Banerjee, L. Colombo, and R. S. Ruoff, *Science*, 2009, **324**, 1312-1314.
27. D. Li, M. B. Müller, S. Gilje, R. B. Kaner, and G. G. Wallace, *Nat. Nanotechnol.*, 2008, **3**, 101-105.
28. H. C. Schniepp, J. L. Li, M. J. McAllister, H. Sai, M. Herrera-Alonso, D. H. Adamson, R. K. Prud'homme, R. Car, D. A. Saville, and I. A. Aksay, *J. Phys. Chem. B*, 2006, **110**, 8535-8539.
29. A. Bagri, C. Mattevi, M. Acik, Y. J. Chabal, M. Chhowalla, and V. B. Shenoy, *Nat. Chem.*, 2010, **2**, 581-587.
30. A. Walther, I. Bjurhager, J. M. Malho, J. Pere, J. Ruokolainen, L. A. Berglund, and O. Ikkala, *Nano Lett.*, 2010, **10**, 2742-2748.
31. M. A. Oneill, D. Warrenfeltz, K. Kates, P. Pellerin, T. Doco, A. G. Darvill, and P. Albersheim, *J. Biol. Chem.*, 1996, **271**, 22923-22930.
32. D. Luo, G. Zhang, J. Liu, and X. Sun, *J. Phys. Chem. C*, 2011, **115**, 11327-11335.
33. I. K. Moon, J. Lee, R. S. Ruoff, and H. Lee, *Nat. Commun.*, 2010, **1**, 73.
34. D. V. Kosynkin, A. L. Higginbotham, A. Sinitskii, J. R. Lomeda, A. Dimiev, B. K. Price, and J. M. Tour, *Nature*, 2009, **458**, 872-876.
35. X. B. Fan, W. C. Peng, Y. Li, X. Y. Li, S. L. Wang, G. L. Zhang, and F. B. Zhang, *Adv. Mater.*, 2008, **20**, 4490-4493.
36. S. F. Pei, and H.-M. Cheng, *Carbon*, 2012, **50**, 3210-3228.
37. C. Li, M. T. Cole, W. Lei, K. Qu, K. Ying, Y. Zhang, A. R. Robertson, J. H. Warner, S. Ding, X. Zhang, B. Wang, and W. I. Milne, *Adv. Funct. Mater.*, 2014, **24**, 1218-1227.
38. X. Lin, P. Liu, Y. Wei, Q. Li, J. Wang, Y. Wu, C. Feng, L. Zhang, S. Fan, and K. Jiang, *Nat. Commun.*, 2013, **4**, 2920.
39. T. Chen, Y. Xue, A. K. Roy, and L. Dai, *ACS Nano*, 2014, **8**, 1039-1046.
40. M. R. Karim, H. Shinoda, M. Nakai, K. Hatakeyama, H. Kamihata, T. Matsui, T. Taniguchi, M. Koinuma, K. Kuroiwa, M. Kurmoo, Y. Matsumoto, and S. Hayami, *Adv. Funct. Mater.*, 2013, **23**, 323-332.
41. H. Liu, L. Zhang, Y. Guo, C. Cheng, L. Yang, L. Jiang, G. Yu, W. Hu, Y. Liu, and D. Zhu, *J. Mater. Chem. C*, 2013, **1**, 3104-3109.

TOC

A facile preparation route for highly conductive borate cross-linked reduced graphene oxide paper

Zhengshan Tian, Chunxiang Xu, Jitao Li, Gangyi Zhu, Jing Wu, Zengliang Shi, Yueyue Wang



A simple evolvement process was used to illustrate the fabrication of GO-based paper with excellent conductivity.